Neutron capture cross section of ^{44}Ti

R. Ejnisman,[1] I. D. Goldman,[2] K. S. Krane,[3,*] P. Mohr,[4] Y. Nakazawa,[5] E. B. Norman,[6] T. Rauscher,[7] and J. Reel[8]
[1]*Department of Physics and Astronomy, University of Rochester, Rochester, New York 14627*
[2]*Instituto de Fisica, Universidade de São Paulo, CP 66318, São Paulo, SP 05389-970, Brazil*
[3]*Department of Physics, Oregon State University, Corvallis, Oregon 97331*
[4]*Institut für Kernphysik, Technische Universität Darmstadt, D-64289 Darmstadt, Germany*
[5]*Department of Physics, State University of New York at Stony Brook, Stony Brook, New York 11974*
[6]*Nuclear Science Division, Lawrence Berkeley National Laboratory, Berkeley, California 94720*
[7]*Institut für Physik, Universität Basel, Basel, Switzerland*
[8]*Department of Physics, Carnegie-Mellon University, Pittsburgh, Pennsylvania 15213*
(Received 20 May 1998)

The cross section for thermal neutron capture by radioactive ^{44}Ti was measured to be $\sigma_\gamma = 1.1 \pm 0.2$ b. This result was shown to be in agreement with a direct capture calculation. Possible implications of the ^{44}Ti(n,γ) reaction in nucleosynthesis are discussed. [S0556-2813(98)04610-X]

PACS number(s): 27.40.+z, 25.40.−h, 26.30.+k

I. INTRODUCTION

Radioactive ^{44}Ti ($N=Z=22$) is produced near the end of the chain of silicon-burning reactions. The presence of this radioisotope in supernova remnants has been confirmed through the observation of the 1157-keV ray from its decay [1], and the half-life of the decay has been recently remeasured to permit a more precise interpretation of this γ-ray flux [2]. ^{44}Ti can also be produced in meteorites through cosmic-ray interactions providing information on solar activity from the cosmic-ray exposure of such objects [3].

The decay of ^{44}Ti eventually leads to stable ^{44}Ca, the abundance of which ought to provide an independent measure of the production of ^{44}Ti in stellar nucleosynthesis. In fact, recent studies in meteorites point to their origin in supernovas by comparing the abundance of Ca isotopes with other isotopes in the same mass region [4]. However, the observed abundances of ^{44}Ca are significantly smaller than the predictions of some stellar models [5]. One possible explanation for this discrepancy is the burnup of ^{44}Ti by neutron capture, since neutron-capture processes are known to be significant in the latter stages of nucleosynthesis.

This possibility motivated a recent attempt to measure the thermal neutron-capture cross section of ^{44}Ti by Ejnisman *et al.* [6]. In that work, they were able to deduce an upper limit to the cross section of 4000 b. Their main difficulties arose from impurities originating from chemical separations. The availability of commercial radioactive sources of ^{44}Ti of exceptional chemical purity provides an opportunity to improve on this result. By choosing the irradiation time to near its optimum for the 3.08-h half-life of ^{45}Ti produced by neutron capture, the required neutron flux to increase the sensitivity over the previous experiment by three to four orders of magnitude can be obtained from a modest research reactor.

The decay schemes of ^{44}Ti and ^{45}Ti are shown in Fig. 1 [7]. The characteristic γ rays of the ^{45}Ti decay, 720 and 1409 keV, are both very weak, being emitted in only about 0.1% of the decays. As a result, it is necessary to rely on the emitted positrons, specifically on the 511-keV γ-ray peak produced by positron annihilation, to signal the presence of ^{45}Ti. Unfortunately, the original ^{44}Sc in equilibrium with

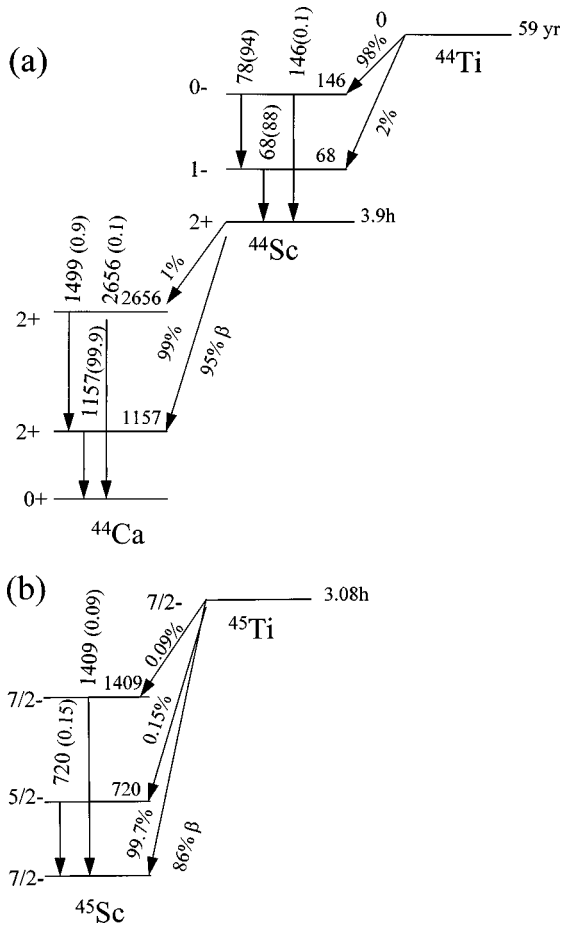

FIG. 1. Partial decay schemes of (a) ^{44}Ti and (b) ^{45}Ti. Energies are given in keV; γ transitions are labeled with their decay intensity. Not to scale.

*Electronic address: kranek@physics.orst.edu

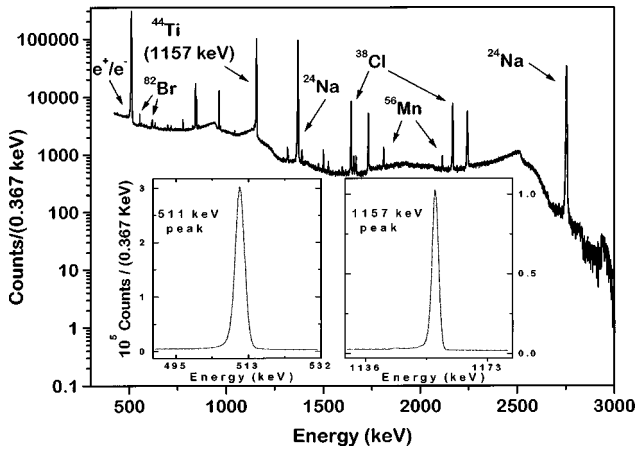

FIG. 2. Typical spectrum obtained following the second irradiation. In the inset, a closer view of the 511- and 1157-keV peaks.

^{44}Ti present in the sample is also a positron emitter, as are certain radioisotopes created upon neutron capture by impurities that are present in the source material or introduced into it during chemical procedures. It is therefore necessary to ''unfold'' the 511-keV peak by subtracting the contributions from ^{44}Ti and positron-emitting impurities to extract its 3.08-h component. To accomplish this subtraction we followed the 511-keV peak over time after the irradiation and used the time dependence of the peak intensity to correct for impurities. The intensity of the resulting 3.08-h component provided a direct measure of the cross section.

II. EXPERIMENTAL DETAILS

There were two separate neutron irradiations, both performed in the thermal column of the Oregon State University 1-MW TRIGA reactor. Gamma rays from the radioactive decays of the samples were observed using an Ortec HPGe detector of 28.8% relative efficiency and 1.70 keV energy resolution [full width at half maximum (FWHM)], both measured for the 1.33-MeV γ ray of ^{60}Co. The Ge detector was surrounded by a low-activity Pb housing. The source-to-detector distance was 10 cm. For data acquisition we used an Ortec ACE system with Maestro software running on a PC. Spectra were accumulated every hour of real time, beginning approximately 1.5 h following the end of the neutron irradiation and continuing for at least 4 days. A typical spectrum obtained following the second irradiation can be observed in Fig. 2.

The ^{44}Ti activity, consisting of 5.0 μCi in 0.2 m*l* of HCl solution, was obtained from Los Alamos National Laboratory. Owing to the necessity of using the positron annihilation γ rays as a signal of the presence of ^{45}Ti, it was necessary to verify that the irradiated sample contained no impurities that could produce positrons, or else that the quantity of any such impurity was sufficiently well known that the total 511-keV peak intensity could be easily and precisely corrected for the effects of the impurities. We therefore made an initial irradiation of about 1/5 of the ^{44}Ti sample (1 μCi) in a neutron flux of 3×10^{12} neutrons/cm^2/s for 1 h. Before the irradiation, the sample was evaporated to dryness; after the irradiation, the sample was redissolved in approximately 0.5 m*l* of 1 mol HCl and transported to the counting system.

Of the impurities known to be present in the sample, only ^{24}Na (resulting from neutron capture by stable ^{23}Na) could be observed at the start of counting. Based on the sample assay, the 1368-keV peak from ^{24}Na ($T_{1/2}=15$ h) was expected to be present in the spectrum at an intensity of 4.5% of the 1157-keV peak from ^{44}Ti, in good agreement with the observed intensity (5.0%). We also observed a very weak impurity of ^{56}Mn, originating from the presence of stable Mn in the original sample.

Based on the examination of the sample following this trial run, we concluded that no impurities decaying by positron emission were present in the sample at the start of the counting period for the first irradiation. However, ^{24}Na can produce positrons through pair production by the 2754-keV γ ray emitted in its decay. The pair production and subsequent positron annihilation can occur anywhere within the liquid sample, its lucite housing, or the Pb shield surrounding the sample and detector, so it was not possible to calculate the contribution of ^{24}Na to the 511-keV peak. We therefore determined its effect empirically by observing the 15-h component in the 511-keV peak.

Once we were satisfied that the impurity question was well understood, the remaining 4 μCi of ^{44}Ti were irradiated for 5 h in a flux of 1.1×10^{13} neutrons/cm^2/s. (The flux was determined by simultaneously irradiating a 66-mg sample of Fe; the intensity of the ^{59}Fe γ rays provided a direct measure of the flux.) One-hour spectra were accumulated for about 5 days. With a source-to-detector distance of 10 cm, the counting system dead time was about 25%. These data were analyzed to determine the cross section of ^{44}Ti.

After a period of about 2 weeks, the 4-μCi sample was irradiated a second time (for 6 h rather than 5 h). This irradiation revealed a greater level of impurities, presumably introduced into the sample through the HCl that was used to dissolve it following the first irradiation. In particular, ^{38}Cl could be observed during the first few 1-h spectra following the irradiation through its 2167-keV γ ray, which can produce positrons by pair production. The intensity of the 2167-keV γ ray from the decay of ^{38}Cl amounted to about 18% of the intensity of the 2754-keV γ ray from ^{24}Na; by estimating the relative probabilities for pair production at these energies we were able to estimate the ^{38}Cl contribution to the 511-keV peak, which amounted to about 15% of the peak intensity (roughly 1.5 standard deviations) in the first 1-h spectrum after the ^{44}Ti and ^{24}Na contributions had been subtracted. The ^{38}Cl contribution was about 6.5% (0.5 standard deviations) in the second 1-h spectrum and negligible thereafter.

Also present in the sample for the second irradiation was a small Br impurity from the HCl, which produced the isotopes ^{80g}Br (17 min), ^{80m}Br (4 h), and ^{82}Br (35 h). ^{82}Br, the activity of which was measured to be 44 nCi based on the counting rate of the 776-keV γ ray, does not produce positrons. ^{80g}Br, calculated to have an activity of 32 nCi based on the ^{82}Br activity, has a weak positron branch (2.6%), but contributes negligibly to the 511-keV peak at the start of counting. ^{80m}Br was expected to have an activity of 0.18 μCi at the start of the measurement, which was con-

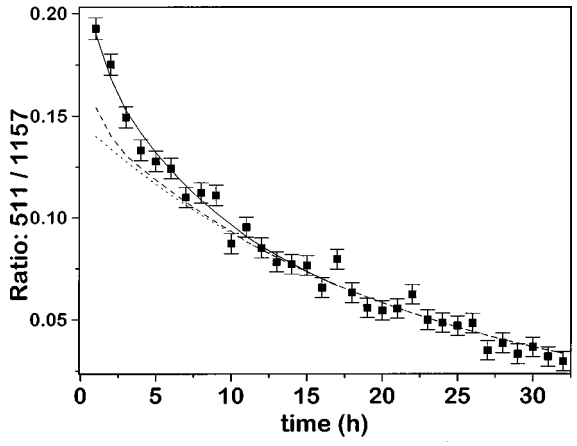

FIG. 3. Time dependence of the ratio of the 511-keV peak to the 1157-keV peak from the second irradiation. The dotted line corresponds to a contribution from ^{24}Na of $\approx$15 h of half-life. The dashed line includes that plus contributions from ^{38}Cl and ^{80}Br. The solid line adds to that the contribution of ^{45}Ti.

sistent with the measured counting rate of the 616-keV γ ray. Although the ^{80m}Br activity was about 3 times the ^{45}Ti activity, its contribution to the 511-keV peak was only about 10% that of the ^{45}Ti, owing to the weak positron branch. We have corrected our data for this contribution, which has been determined from the measured intensity of the 776-keV γ ray from ^{82}Br.

III. RESULTS AND ANALYSIS

As mentioned above, the characteristic γ rays from ^{45}Ti were too weak to grant a direct observation of that isotope after neutron activation of the ^{44}Ti target. Based on the known branching ratios of the 720- and 1409-keV transitions and the measured thermal neutron flux, we deduce from their absence that the neutron cross section must be less than 3 b.

In order to eliminate possible systematic errors due to variations in the live timer of our analog-to-digital converter (ADC), we normalized the 511-keV peak intensities in each 1-h run using the intensity of the 1157-keV γ ray from the decay of ^{44}Ti. Owing to its long half-life of 60.4 ± 1.4 yr (unweighted average from works of Ref. [2]), the ^{44}Ti decay can be regarded as occurring at a constant rate during the course of our 5-day experiment.

Because the γ-ray peaks in the spectrum are well isolated from one another, it was not necessary to use peak fitting to determine the peak areas. Instead, we used a simpler summing procedure after subtracting a linear background. Background corrections were relatively unimportant for the 511- and 1157-keV peaks; the ratio of peak area to background area was greater than 20:1.

The base line 511/1157 ratio was determined from a series of runs taken at least 4 days after the irradiation. This ratio was 3.424(1) for the first irradiation and 3.460(1) for the second irradiation. These values agree with the calculated value of 3.45 based on the decay parameters and our measured detector efficiencies (determined using a source of ^{152}Eu). Subtracting the base line 511/1157 ratio from the data, we obtain the results shown in Fig. 3 for the first 35 h of counting after the second irradiation. In the figure, the dotted line represents the contribution of a 15-h component due to ^{24}Na, whose amplitude was obtained from runs 15–35. The dashed line shows the expected contribution of ^{38}Cl and ^{80m}Br added to that of ^{24}Na. The remaining 511-keV counts agree quite well with a contribution of ^{45}Ti, as can be seen from the solid line, which corresponds to a fit with a fixed 3.08-h half-life.

The cross section for the ^{44}Ti(n,γ) reaction can then be extracted from the ratio r_i of the 511-keV ^{45}Ti γ-ray and the 1157-keV ^{44}Ti γ-ray intensities. In any particular 1-h run beginning at time t_i (with $t_i=0$ defining the start of counting) r_i is given by

$$r_i=\frac{I_i(511)}{I_i(1157)}=\frac{a_{45}e^{-\lambda_{45}t_i}\epsilon(511)b_{45}(511)f_{45}}{a_{44}\epsilon(1157)b_{44}(1157)f_{44}}, \qquad (1)$$

where a_A is the activity of isotope A of decay rate λ_A at $t_i=0$ and $\epsilon(E_\gamma)$ represents the detector efficiency at energy E_γ of branching ratio $b_A(E_\gamma)$. The decay factor f_A corrects for the decrease in the amount of the isotope A during the 1-h counting intervals ($f_{44}=1.000$, $f_{45}=0.895$).

The thermal neutron capture cross section σ_γ at a constant flux ϕ can now be obtained from

$$\sigma_\gamma=\frac{\lambda_{44}b_{45}(511)\epsilon(1157)b_{44}(1157)\langle r_i/e^{-\lambda_{45}t_i}\rangle}{\phi(1-e^{-\lambda_{45}t_b})e^{-\lambda_{45}t_d}f_{45}b_{44}(511)\epsilon(511)b_{44}(511)}, \qquad (2)$$

where the angular brackets denote an average over the data-acquisition runs, t_b is the neutron bombardment time, and t_d is the delay between the end of bombardment and the start of counting.

From the first irradiation, with $\langle r_i/e^{-\lambda_{45}t_i}\rangle=0.056$, we obtain $\sigma_\gamma=1.25$ b, and from the second irradiation, with $\langle r_i/e^{-\lambda_{45}t_i}\rangle=0.041$, we obtain $\sigma_\gamma=0.93$ b. The statistical uncertainty associated with each result is $\pm10-15\%$. Including the $\pm10\%$ uncertainty in the measured neutron flux, we obtain the final result for the cross section:

$$\sigma_\gamma=1.1\pm0.2\,\text{b}.$$

Our data also permit a determination of the cross section of the (n,p) reaction on ^{44}Ti, which would lead to 3.9 h ^{44}Sc. Because ^{44}Sc is also produced following the decay of ^{44}Ti, the 1157-keV transition emitted in the ^{44}Sc decay could thus show two components: the 59-yr component from the ^{44}Ti $\rightarrow$ ^{44}Sc decay and the 3.9-h component from the ^{44}Sc newly produced through the (n,p) reaction. Using the MCA live timer for normalization, we have examined the 1157-keV intensity to search for the presence of a 3.9-h component in the first 10 h following the irradiation. At most, only a very weak 3.9-h component could be identified, from which we conclude

$$\sigma_p<0.2\text{ b}.$$

The possible presence of this weak 3.9-h component in the 1157-keV intensity does not alter our previous conclusions for the (n,γ) cross section.

IV. THEORETICAL ANALYSIS AND DISCUSSIONS

In the following section we calculate the neutron-capture cross section of the reaction $^{44}\mathrm{Ti}(n,\gamma)^{45}\mathrm{Ti}$ using the direct-capture (DC) model and the statistical Hauser-Feshbach model, and we discuss the applicability and accuracy of both models for this reaction. As will be shown, the cross section exhibits a pure $1/v$ behavior near the experimental energy. However, the total cross section (i.e., sum of direct capture and resonant or Hauser-Feshbach contributions) will change as a function of energy in the following way: at thermal and very low energies it shows the above-mentioned $1/v$ behavior; up to 8 keV it exhibits single resonance structures and starting from 8 to 9 keV (up to about 1 MeV) it shows a $1/v$ behavior again but ''shifted'' with respect to the DC contribution because of the many resonances.

A. Direct-capture calculations

The DC calculations were performed similar to Ref. [8], and the DC formalism was taken from Ref. [9]. The DC cross section $\sigma_\gamma^{\mathrm{DC}}$ is given by the sum over all partial transitions $\sigma_{\gamma,i}^{\mathrm{DC}}$:

$$\sigma_\gamma^{\mathrm{DC}} = \sum_i (C^2S)_i \sigma_{\gamma,i}^{\mathrm{DC}}, \tag{3}$$

where C^2S_i is the spectroscopic factor of the ith level which is a measure of the probability to find the nucleus ^{45}Ti in a $^{44}\mathrm{Ti}\otimes n$ single-particle configuration. The $\sigma_{\gamma,i}^{\mathrm{DC}}$ depend on the overlap integrals

$$I_{l_b j_b; l_a j_a}^{E\mathcal{L}/M\mathcal{L}} = \int dr\, u_{l_b j_b}(r) \mathcal{O}^{E\mathcal{L}/M\mathcal{L}}(r)\, \chi_{l_a j_a}(r), \tag{4}$$

with the scattering wave function $\chi_{l_a j_a}(r)$, the bound state wave function $u_{l_b j_b}(r)$, and the electromagnetic transition operators $\mathcal{O}^{E\mathcal{L}/M\mathcal{L}}$ of order $E\mathcal{L}$ and $M\mathcal{L}$.

The basic ingredient for the calculation of the wave functions is the $n+^{44}$Ti potential. Because of the small number of adjustable parameters of folding potentials and because of the successful application to thermal and thermonuclear neutron capture (e.g., Ref. [8]), we first calculate the density of ^{44}Ti which is necessary for the calculation of the folding integral. We applied the procedure of Abele and Staudt [10] which was used for the nucleus $^{20}\mathrm{Ne}=^{16}\mathrm{O}\otimes\alpha$ in that work. In our calculation ^{44}Ti is composed of a ^{40}Ca core, an α particle, and the 0^+ ground state wave function with 12 oscillator quanta (3 quanta per each nucleon outside the ^{40}Ca core in the fp shell) which was taken from [13]. The resulting density of ^{44}Ti has a root-mean-square radius of $r_{\mathrm{rms}} = 3.49$ fm which is slightly larger than ^{40}Ca ($r_{\mathrm{rms}} = 3.39$ fm). The folding potential is given by [11]

$$V(R) = \lambda\, V_{\mathrm{F}}(R) = \lambda \int\int \rho_a(\mathbf{r}_1)\rho_A(\mathbf{r}_2)\, v_{\mathrm{eff}}(E,\rho_a,\rho_A,s)\, d\mathbf{r}_1 d\mathbf{r}_2, \tag{5}$$

with λ being a potential strength parameter close to unity, and $s=|\mathbf{R}+\mathbf{r}_2-\mathbf{r}_1|$, where R is the separation of the centers of mass of the projectile and the target nucleus. The effective nucleon-nucleon interaction v_{eff} has been taken in the DDM3Y parametrization [12]. The resulting folding potential has a volume integral per interacting nucleon pair, $J_R = 501.2$ MeV fm^3 ($\lambda=1$), and a rms radius $r_{\mathrm{rms}} = 4.22$ fm.

The potential strength parameter λ is adjusted to the scattering length b (incoming s wave at thermal energies) and to the binding energy E_{Bi} of the ith bound state wave function. Because b is not measured for neutron scattering on ^{44}Ti, we adjusted the parameter λ to the scattering length of ^{42}Ca which has, at least in a simple shell model, the same neutron configuration as ^{44}Ti. This adjustment also compensates the uncertainties from the determination of the ^{44}Ti density. From $b_{\mathrm{bound}}(^{42}\mathrm{Ca}) = 3.36$ fm [$b_{\mathrm{free}}(^{42}\mathrm{Ca}) = 3.31$ fm] [14] one obtains $\lambda = 0.853$. A similar result is obtained from the average of the neighboring Ti isotopes ^{46}Ti and ^{48}Ti; we adopt $\lambda = 0.855 \pm 0.050$ for the following calculations.

In principle, for the calculation of the neutron capture cross section of ^{44}Ti, one has to take into account all bound states of ^{45}Ti below the neutron threshold at $E_x = 9530$ keV [15]. However, it has been shown for the reaction $^{48}\mathrm{Ca}(n,\gamma)^{49}\mathrm{Ca}$ that the $E1$ transitions to the bound p waves are dominating, and a similar behavior is expected for ^{44}Ti, where the neutrons have also to be included in the fp shell. The spectroscopic factors C^2S of all bound states of ^{45}Ti are not known experimentally, but shell model calculations indicate that most of the p-wave strength is located in a few low-lying levels [16].

We have performed calculations for the two extreme cases.

(i) The first $1/2^-$ and $3/2^-$ levels which are experimentally known [$E_{x,1}(1/2^-) = 1799.2$ keV, $E_{x,1}(3/2^-) = 36.7$ keV [17]] contain the full spectroscopic strength [$C^2S(1/2^-) = C^2S(3/2^-) = 1.0$]. This leads to an upper limit for the capture cross section because the capture cross section increases with increasing transition energy.

(ii) The $1/2^-$ and $3/2^-$ strength is uniformly distributed from the energy $E_{x,1}$ of the first experimentally known $1/2^-$ and $3/2^-$ levels, respectively, up to the neutron threshold [$\Phi(E) = \mathrm{const}$]. Because of the E_γ^3 dependence of the $E1$ transition probability, this leads to an average transition energy of

$$\overline{E_\gamma^3} = \int_0^{E_{\gamma,\max}} E_\gamma^3 \Phi(E_\gamma) dE_\gamma \Big/ \int_0^{E_{\gamma,\max}} \Phi(E_\gamma) dE_\gamma = E_{\gamma,\max}^3/4 \tag{6}$$

to an effective final state with $E_{B,\mathrm{eff}} = \sqrt[3]{\overline{E_\gamma^3}}$ and with the full spectroscopic strength $C^2S = 1.0$. $E_{\gamma,\max}$ is the maximum transition energy given by the difference between the binding energy $E_B = 9530$ keV of the ground state and the excitation energy $E_{x,1}$.

The results of the calculations for cases (i) and (ii) are listed in Table I; they differ only by about 20%. At first view this small difference is unexpected because of the strong E_γ^3 energy dependence of the transition probability. However, lower transition energies E_γ correspond to smaller binding energies E_B, and this leads to a slower decay of the bound state wave function towards larger radii. Because the main

TABLE I. Calculated DC cross section $\sigma_\gamma^{\mathrm{DC}}$ of the reaction $^{44}\mathrm{Ti}(n,\gamma)^{45}\mathrm{Ti}$ at the thermal energy $E=25.3$ meV. Cases (i) and (ii) refer to Sec. IV A.

	Case (i)		Case (ii)	
Transition	$E_\gamma = E_{\gamma,\max}$ (keV)	$\sigma_\gamma^{\mathrm{DC}}$ (mb)	$E_\gamma = E_{\gamma,\max}/\sqrt[3]{4}$ (keV)	$\sigma_\gamma^{\mathrm{DC}}$ (mb)
$s \rightarrow 1/2^-$	7730.8	313.5	4870.1	233.3
$s \rightarrow 3/2^-$	9493.3	660.3	5980.4	544.3
Sum	Upper limit:	973.8		777.6

contribution of the DC cross section in the integrand of Eq. (4) comes from the nuclear surface around 5–10 fm (the maximum of the integrand is at $r \approx 6.5$ fm), the lower transition probability is compensated by a larger value of the bound state wave function. Additionally, in the case of the $^{44}\mathrm{Ti}(n,\gamma)^{45}\mathrm{Ti}$ reaction a cancellation between the positive and negative regions of the integrand of Eq. (4) enhances the cross section at smaller transition energies.

Taking into account the uncertainties of the spectroscopic factors and the spectroscopic strength, respectively, and the uncertainties of the optical potential (parameter λ), the final result of the DC calculations at thermal energies is

$$\sigma_\gamma^{\mathrm{DC}} = 0.8 \pm 0.2 \text{ b},$$

which is in reasonable agreement with the experimental value $\sigma_{\mathrm{expt}} = 1.1 \pm 0.2$ b.

At thermonuclear energies the *s*-wave contribution of the capture cross section can easily be calculated using the well-known $1/v$ law. However, for several nuclei a significant or even dominating *p* wave contribution of $E1$ transitions from the incoming *p*-wave to bound *s* and *d* waves was found in the keV region (e.g., ^{12}C [18], ^{15}N [19], ^{26}Mg [20], etc.). This *p*-wave contribution is roughly proportional to v instead of $1/v$. For the neighboring nucleus ^{48}Ca such a *p*-wave contribution was not found [8], and our calculations indicate that the *p*-wave contribution is practically negligible for ^{44}Ti, too.

In conclusion, the calculated DC cross section of ^{44}Ti shows almost pure $1/v$ behavior with a value of $\sigma_\gamma^{\mathrm{DC}} = 0.8 \pm 0.2$ b at the thermal energy $E = 25.3$ meV.

B. Statistical model calculations

While DC dominates the cross section in the absence of resonances, compound nucleus formation is favored in the region of higher level density. The statistical model [Hauser-Feshbach (HF)] [21], which averages over resonances, is used to describe the majority of reactions at astrophysical energies [22,23]. The necessary condition for its application to calculate astrophysical reaction rates is a sufficient number of resonances in the contributing energy window [24]. In the case of neutron capture on ^{44}Ti, it can be estimated [24] that the statistical model is applicable at energies above about 9 keV. Therefore, in order to compute reaction rates at stellar temperatures, one has to invoke a statistical model calculation.

For the calculation, we utilized the code NON-SMOKER [25] which is an improved Hauser-Feshbach code based on the well-known code SMOKER [26]. Of all nuclear properties entering the calculation, in this context the nuclear masses, level densities, and the neutron-nucleus optical potential are among the most important. Nuclear masses were taken from experiment [27]. The nuclear level density was calculated in a recently improved description [24] within the framework of the back-shifted Fermi-gas approach, including an energy-dependent level density parameter *a* and taking into account thermal damping of shell effects. For a detailed description of the neutron transmission coefficients involved, see [24] and references therein. Low-lying bound states in ^{45}Ti are experimentally known [17] and included in the calculation. The code also treats width fluctuation corrections but they are not of importance in the present context.

The results of the calculation are shown in Tables II and III. Comparing the HF cross section of 49 mb at 30 keV to the $1/v$ DC cross section, we find that the HF contribution is larger by almost two orders of magnitude and that the DC contribution can be neglected at this energy, as expected.

When comparing our HF results to that of a previous HF calculation [22], we find that our value is larger by a factor of about 2.2. This is mainly due to the different treatment of the level density and also because we use more realistic optical potentials as compared to the equivalent square well potentials used in Ref. [22].

C. Discussion

Following the excitation curve of the reaction $^{44}\mathrm{Ti}(n,\gamma)^{45}\mathrm{Ti}$ from thermal to thermonuclear energies, one

TABLE II. Calculated HF cross sections of $^{44}\mathrm{Ti}(n,\gamma)^{45}\mathrm{Ti}$.

$E_{\mathrm{c.m.}}$ [MeV]	Cross section [b]
0.010	8.535×10^{-2}
0.057	3.499×10^{-2}
0.113	2.549×10^{-2}
0.200	2.008×10^{-2}
0.311	1.687×10^{-2}
0.518	1.354×10^{-2}
0.808	1.096×10^{-2}
1.023	9.723×10^{-3}
1.514	5.103×10^{-3}
2.088	4.219×10^{-3}
2.574	3.541×10^{-3}
3.005	2.970×10^{-3}
3.502	2.576×10^{-3}
4.076	2.212×10^{-3}
4.508	1.982×10^{-3}
5.238	1.755×10^{-3}

TABLE III. Astrophysical reaction rates $N_A\langle\sigma v\rangle$ of ^{44}Ti$(n,\gamma)^{45}$Ti. The *ground* rate is for the target in the ground state; the *stellar* rate is for a thermally excited target ^{44}Ti.

Temperature [10^9 K]	Rate [10^6 cm^3 s^{-1} mol^{-1}]	
	Ground	Stellar
0.10	7.88	7.88
0.20	7.34	7.34
0.30	7.24	7.24
0.40	7.21	7.21
0.50	7.22	7.22
1.00	7.36	7.36
1.50	7.52	7.52
2.00	7.64	7.61
2.50	7.71	7.61
3.00	7.74	7.50
3.50	7.73	7.30
4.00	7.69	7.04
4.50	7.63	6.73
5.00	7.56	6.40
6.00	7.39	5.72
7.00	7.21	5.08
8.00	7.03	4.51
9.00	6.85	4.02
10.00	6.69	3.61

passes through three different regimes [28], characterized by different level densities. At thermal energy, the cross section is dominated by a nonresonant direct-capture contribution which may interfere with a few single, widely spaced resonances. The fact that the experimental thermal capture cross section can be described successfully using the DC model indicates that there are no significant resonant contributions at this energy. As found from our calculations, the DC cross section will fall off as $1/v$ at slightly higher energies.

At energies above 9 keV the level density is so high that many resonances overlap and the cross section can be calculated by an average over many resonances. Again, this average shows the well-known $1/v$ behavior because of the domination of the $E1$ transitions but quantitatively it is higher by two orders of magnitude than the DC cross section due to the resonant contributions.

The intermediate region between thermal energies and 8–9 keV exhibits a complicated structure given by the coherent sum of a nonresonant DC background and the contributions of resonances with on average gradually decreasing spacing. For a proper treatment, information on states in ^{45}Ti above the neutron separation energy ($S_n = 9.53$ MeV) would have to be included but is currently not available.

V. CONCLUSION

We have for the first time measured the thermal neutron-capture cross section of the radioactive ^{44}Ti nucleus. Our result of $\sigma_\gamma = 1.1 \pm 0.2$ b is in agreement with direct-capture calculations. We expect, however, that, at stellar temperatures, the thermal neutron-capture rate becomes dominated by a resonant contribution larger than the $1/v$ term by about two orders of magnitude.

From the astrophysical point of view, enhancing the accuracy of the ^{44}Ti(n,γ) rates still leaves the uncertainties in the α-capture reaction chain which produces ^{44}Ti in explosive Si burning [29,30]. Recent work [31,25] indicates that the uncertainties in those α-capture reactions on self-conjugate ($N=Z$) targets could be larger than those from the (n,γ) reactions and account for most of the uncertainty in the final ^{44}Ti abundance. We also note that a recent investigation by The *et al.* [32] suggests that the ^{44}Ti(n,γ) reaction does *not* play a crucial role in the nucleosynthesis of ^{44}Ti. However, it is still possible that in cases where exceptionally large neutron fluxes are present, the neutron-capture cross section of ^{44}Ti still does consist of an essential piece of the nucleosynthesis puzzle. One possible example is the $n\beta$ process of Ref. [33], which was conceived to explain isotopic anomalies in the Ca-Ti mass region favoring isotopes of large N.

To conclude, we hope the experimental part of this work serves as a motivation for more investigations utilizing the elusive, but interesting, radioactive targets, and that the theoretical analysis helps to shed more light into models of nucleosynthesis that involve the ^{44}Ti(n,γ) reaction.

ACKNOWLEDGMENTS

We are grateful to the staff of the Oregon State University Radiation Center for their hospitality and assistance in performing the irradiations, sample handling, and counting. Y.N. and J.R. acknowledge support from the Research Experiences for Undergraduates program of the National Science Foundation (NSF Grant No. PHY-9531528); R.E. acknowledges the financial support from CNPq, NSF (Grant No. PHY-9457897) and the David and Lucile Packard Foundation. This work was supported in part by Oregon State University and in part by the U. S. Department of Energy under contracts DE-FG03-98ER41060 (Oregon State University) and DE-AC03-76SF00098 (Lawrence Berkeley National Laboratory).

[1] A. F. Iyudin *et al.*, Astron. Astrophys. **284**, L1 (1994).

[2] E. B. Norman, E. Browne, Y. D. Chan, I. D. Goldman, R. M. Larimer, K. T. Lesko, M. Nelson, F. E. Wietfeldt, and I. Zlimen, Phys. Rev. C **57**, 2010 (1998); J. Görres *et al.*, Phys. Rev. Lett. **80**, 2554 (1998); I. Ahmad, G. Bonino, G. C. Castagnoli, S. M. Fischer, W. Kutschera, and M. Paul, *ibid.* **80**, 2550 (1998).

[3] G. Bonino, G. C. Castagnoli, N. Bhandari, and C. Taricco, Science **270**, 1648 (1995).

[4] S. Amari and E. Zinner, in *Astrophysical Implications of the*

Laboratory Study of Presolar Materials, edited by T. J. Bernatowicz and E. Zinner, AIP Conf. Proc. No. 402 (AIP, New York, 1997), 287.
[5] S. E. Woosley, W. D. Arnett, and D. D. Clayton, Astrophys. J., Suppl. **26**, 231 (1973).
[6] R. Ejnisman, I. D. Goldman, P. R. Pascholati, M. T. F. da Cruz, R. M. Oliveira, P. B. Rios, and R. T. dos Santos, Nuovo Cimento A **109**, 1461 (1996).
[7] R. B. Firestone and V. S. Shirley, *Table of Isotopes* (Wiley, New York, 1996).
[8] H. Beer, C. Coceva, P. V. Sedyshev, Yu. P. Popov, H. Herndl, R. Hofinger, P. Mohr, and H. Oberhummer, Phys. Rev. C **54**, 2014 (1996).
[9] K. H. Kim, M. H. Park, and B. T. Kim, Phys. Rev. C **35**, 363 (1987).
[10] H. Abele and G. Staudt, Phys. Rev. C **47**, 742 (1993).
[11] G. R. Satchler and W. G. Love, Phys. Rep., Phys. Lett. **55C**, 183 (1979).
[12] A. M. Kobos, B. A. Brown, R. Lindsay, and G. R. Satchler, Nucl. Phys. **A425**, 205 (1984).
[13] U. Atzrott, P. Mohr, H. Abele, C. Hillenmayer, and G. Staudt, Phys. Rev. C **53**, 1336 (1996).
[14] V. F. Sears, Neutron News **3**, 26 (1992).
[15] G. Audi and A. H. Wapstra, Nucl. Phys. **A565**, 1 (1993).
[16] W. A. Richter, M. G. Van der Merwe, R. E. Julies, and B. A. Brown, Nucl. Phys. **A577**, 585 (1994).
[17] Data base ENSDF, NNDC, Brookhaven National Laboratory, Upton, NY.
[18] T. Ohsaki, Y. Nagai, M. Igashira, T. Shima, K. Takeda, S. Seino, and T. Irie, Astrophys. J. **422**, 912 (1994).
[19] J. Meissner, H. Schatz, H. Herndl, M. Wiescher, H. Beer, and F. Käppeler, Phys. Rev. C **53**, 977 (1996).
[20] P. Mohr, H. Beer, H. Oberhummer, and G. Staudt, Phys. Rev. C **58**, 931 (1998).
[21] W. Hauser and H. Feshbach, Phys. Rev. **87**, 366 (1952).
[22] S. E. Woosley, W. A. Fowler, J. A. Holmes, and B. A. Zimmerman, At. Data Nucl. Data Tables **22**, 371 (1978).
[23] J. J. Cowan, F.-K. Thielemann, and J. W. Truran, Phys. Rep. **208**, 267 (1991).
[24] T. Rauscher, F.-K. Thielemann, and K.-L. Kratz, Phys. Rev. C **56**, 1613 (1997).
[25] T. Rauscher and F.-K. Thielemann, in *Atomic and Nuclear Astrophysics*, edited by A. Mezzacappa (IOP, Bristol, in press).
[26] F.-K. Thielemann, M. Arnould, and J. W. Truran, in *Advances in Nuclear Astrophysics*, edited by E. Vangioni-Flam (Editions Frontière, Gif-sur-Yvette, 1987), p. 525.
[27] G. Audi and A. H. Wapstra, Nucl. Phys. **A595**, 409 (1995).
[28] R. V. Wagoner, Astrophys. J., Suppl. **18**, 247 (1969).
[29] S. E. Woosley and T. A. Weaver, Astrophys. J., Suppl. Ser. **101**, 181 (1995).
[30] F.-K. Thielemann, K. Nomoto, and M. Hashimoto, Astrophys. J. **460**, 408 (1996).
[31] R. D. Hoffman, S. E. Woosley, T. A. Weaver, T. Rauscher, and F.-K. Thielemann (unpublished).
[32] L. S. The, D. D. Clayton, L. Jin, and B.S. Meyer, Astrophys. J. (submitted).
[33] D. G. Sandler, S. E. Koonin, and W. A. Fowler, Astrophys. J. **259**, 908 (1982).